Oral Microbiology Immunology 2004: 19: 144–149
Printed in Denmark. All rights reserved

Oral Microbiology and Immunology

Treponema denticola immunoinhibitory protein induces irreversible G_1 arrest in activated human lymphocytes

W. Lee, L. Pankoski, A. Zekavat, B. J. Shenker
Department of Pathology, University of Pennsylvania School of Dental Medicine, Philadelphia, PA, USA

Lee W, Pankoski L, Zekavat A, Shenker BJ. Treponema denticola *immunoinhibitory protein induces irreversible G_1 arrest in activated human lymphocytes. Oral Microbiol Immunol 2004: 19: 144–149.* © Blackwell Munksgaard, 2004.

Oral spirochetes may contribute to the pathogenesis of a number of disorders including periodontal and periradicular diseases; however, the mechanism (s) by which these organisms act to cause disease is unknown. We have previously shown that extracts of the oral spirochete, *Treponema denticola,* contain an immunosuppressive protein (Sip) which impairs human lymphocyte proliferation. The objective of this study was to determine the mechanism by which Sip alters the proliferative response of lymphocytes. Human T-cells were activated by PHA in the presence or absence of Sip and cell cycle progression was assessed by flow cytometry. Cell cycle distribution was based upon DNA, RNA and protein content as well as expression of the activation markers; CD69 and IL-2R. Seventy-two hours following activation with PHA, cells were found in the G_0, G_1, S and G_2/M phases of the cell cycle. In contrast, pretreatment with Sip resulted in a significant reduction of cells in the S and G_2/M phases and a concomitant increase in the G_1 phase. Sip did not alter the expression of the early activation markers CD69 and CD25R. To determine if G_1 arrest resulted in activation of the checkpoint and cell death, we also monitored Sip-treated cells for apoptosis. Indeed, treatment with Sip resulted in both DNA fragmentation and caspase activation after 96 h. Our results indicate that Sip induces G_1 arrest in human T-cells and, furthermore, that the arrest is irreversible, culminating in activation of the apoptotic cascade. We propose that if cell cycle arrest occurs *in vivo*, it may result in local and/or systemic immunosuppression and thereby enhance the pathogenicity of spirochetes and/or that of other opportunistic organisms.

Key words: lymphocytes; bacteria; spirochetes; periodontitis; immunosuppression

B. J. Shenker, Department of Pathology, University of Pennsylvania School of Dental Medicine, 240 South 40th Street, Philadelphia, PA 19104-6030, USA
Tel.: +1 215 898 5959; fax: +1 215 573 2050;
e-mail: shenker@pobox.upenn.edu
Accepted for publication October 30, 2003

Spirochetes are motile, gram-negative, anaerobic organisms which have been implicated as pathogens in several human infections including syphilis, yaws and Lyme disease as well as periodontal disease and periapical infections. Spirochetes are conspicuous inhabitants of subgingival plaque in patients with gingivitis and periodontitis (19). Moreover, the presence of the oral spirochete, *Treponema denticola*, has been associated with the severity of periodontal disease (1, 20). Recent studies also suggest that, in addition to periodontal diseases, spirochetes may also be involved in pulpal and periapical infections (22, 37). For instance, *T. denticola* accounted for more than 50% of the flora in infected root canals and in acute alveolar abscesses (35, 36). It is not clear how spirochetes contribute to the pathogenesis of these disorders. However, several potential virulence factors have been described, including adherence factors, cytopathic factors, chemotactic factors and a number of surface structures (3, 14, 26, 38).

It is also well known that several infectious diseases are associated with pathogens capable of impairing immunologic responsiveness; these include measles, leprosy, candidiasis, leishmaniasis, syphilis, certain forms of periodontal diseases as well as pulpal and periapical diseases (28, 36). In fact, several microorganisms such as *Actinobacillus actinomycetemcomitans* (30, 31), *Fusobacterium nucleatum* (29, 40), *T. denticola* (32), *Vibrio cholera* (13), group A streptococcus (10, 21),

Pseudomonas aeruginosa (9), *Plasmodium berghei* (17), rubella, influenza, polio and parvovirus (8, 15, 16, 24) have been shown to produce immunosuppressive factors. These immunomodulatory agents may act by interfering with either the induction or the expression of the immune response. Collectively, these studies illustrate the potential of bacteria and/or bacterial products to act as exogenous immunoregulatory agents that could have profound effects on the course of infection. In this regard, we previously demonstrated that soluble sonic extracts of several strains of *T. denticola* inhibit human peripheral blood lymphocyte (HPBL) proliferative responses to both mitogens and antigens *in vitro* (32). These effects were found to be due to a protein composed of two polypeptides of 50 and 56 kDa and were designated spirochete immunoinhibitory protein (Sip). The objective of this study was to determine the mechanism by which Sip impairs lymphocyte responsiveness.

Materials and methods

Bacterial cultures and sonic extract preparation

Spirochete strain LL2513 was used for this study. Bacteria were grown in 500 ml of TYGVS (Trypticase, yeast extract, glucose, volatile fatty acids, serum) spirochete medium containing veal infusion broth (Difco Laboratories, Detroit, MI) supplemented with yeast extract (BBL), trypticase peptone, ammonium sulfate, L-cysteine hydrochloride, glucose, and volatile fatty acid solution (acetic acid, propionic acid, *n*-butyric acid, *n*-valeric acid, isobutyric acid, isovaleric acid and D,L-methylbutyric acid in dH_2O (32). Cultures were incubated under anaerobic conditions (95% N_2 and 5% CO_2). After 72 h, bacterial cell suspensions were harvested, washed in phosphate-buffered saline (PBS) containing PMSF, and disrupted by sonication in the presence of an equal volume of glass beads. The equivalent of 1 liter of washed spirochetes was sonicated (Sonic Dismembrator, Model 550, Fisher Scientific, Pittsburgh, PA) for a total of 7 min with 30-s pulses. Cellular debris was removed by centrifugation at 12 000 ***g*** for 20 min and the membrane fraction was sedimented by ultracentrifugation at 85 000 ***g*** for 60 min at 4°C. The supernatant was dialyzed against PBS and sequentially fractionated using ion exchange, chromatofocusing and gel filtration chromatography. Column fractions were screened for their ability to inhibit Con-A-induced ^{3}H-thymidine incorporation in human lymphocytes (see below).

Cell cultures

Human peripheral blood mononuclear cells (HPBMC) were prepared by buoyant density centrifugation on Ficoll-Hypaque (Amersham Pharmacia Biotech, Piscataway, NJ) as previously described (30). HPBMC were washed twice with Hanks' balanced salt solution and diluted to 2.0×10^6 viable cells per ml culture medium consisting of RPMI 1640, 2% penicillin/streptomycin, and 2% heat-inactivated human AB serum. Cell cultures (2×10^5 HPBMC) were prepared in flat-bottomed 96-well microculture plates. Each culture received 0.1 ml of cells and 0.1 ml of medium or 0.1 ml of varying concentration of Sip diluted in medium. The cells were incubated for 30 min at 37°C and then an optimal mitogenic dose of Con A (1 μg/culture; Calbiochem, La Jolla, CA) was added. The cells were incubated for 72 h, and DNA synthesis was assessed by the incorporation of (^{3}H)-thymidine.

Cell cycle analysis was performed on HPBMC by a modification of the method of Schmid et al. (25). Briefly, 1-ml cultures (2×10^6 cells) were incubated for 72 h in the presence of medium, PHA (1 μg/ml; Murex, Dartfield, UK) or PHA and Sip. Cells were harvested, washed with Hanks' balanced salt solution containing 1% AB serum and resuspended in 1 ml of 80% ice cold ethanol for 2 h at –20°C. The cells were stained with 10 μg/ml of propidium iodide (Sigma Chemical Co., St Louis, MO) for 30 min and analyzed on a Becton-Dickinson FACStar^{PLUS} flow cytometer. Propidium iodide fluorescence was excited by an argon laser operating at 488 nm and fluorescence was measured with a 630/22-nm bandpass filter using linear amplification.

To distinguish between the G_0 and G_1 phases of the cell cycle, multiparametric cell cycle analysis was employed; total RNA and protein content in relation to cell cycle were assessed. Cells were washed in PBS, fixed in 1 ml of 80% ice cold ethanol, and stained with pyronin Y (4 μg/ml; Sigma Chemical Co) or FITC (0.1 μg/ml; Molecular Probes, Eugene, OR) to measure RNA or protein content, respectively. DNA content was measured with Hoechst 33342 (2 μg/ml; Molecular Probes) and the cells were analyzed by flow cytometry. Hoechst 33342 fluorescence was excited with one laser operating in ultraviolet emission and fluorescence was detected through a 424/44-nm bandpass filter. Both pyronin Y and FITC were excited with a second laser operating at 488 nm, and fluorescence was measured with a 575/26-nm bandpass filter or a 535/30-nm bandpass filter, respectively.

Analysis of cell activation markers

HPBMC (2×10^6/ml) were incubated for 24 h with PHA in the presence or absence of Sip. The cells were washed with Hanks' balanced salt solution containing 1% BSA and 0.1% sodium azide. Cells were then stained with anti-CD25 or anti-CD69 monoclonal antibodies conjugated to fluorescein isothiocyanate ((FITC); Becton Dickinson Immunocytometry Systems; San Jose, CA). After incubation on ice for 15 min, cells were washed, fixed in 1% paraformaldehyde and analyzed by flow cytometry. To identify T-cells, samples were also stained with anti-CD3 monoclonal antibody conjugated to phycoerythrin (Becton Dickinson Immunocytometry Systems). Cells which gave fluorescence signals brighter than those observed for 98% of control cells were considered to be positive.

Analysis of apoptosis

Apoptosis was monitored by measuring DNA fragmentation (TUNEL assay) and caspase activation. HPBMC were incubated with PHA in the presence or absence of Sip for 96 h. For the TUNEL assay, cells were harvested, washed with 2 ml of PBS containing 1% BSA and centrifuged at 300 ***g*** for 10 min. Cells were then fixed in 4% paraformaldehyde for 30 min at room temperature. After washing, cells were permeabilized in dH_2O containing

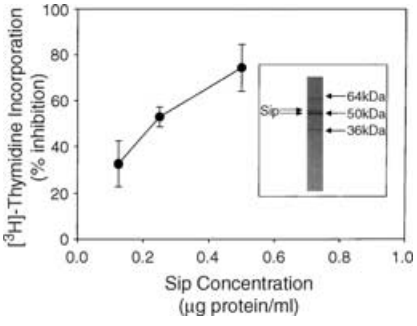

Fig. 1. Effect of Sip on lymphocyte proliferation. HPBMC were incubated with varying amounts of Sip (μg protein/ml) for 30 min followed by the addition of Con A. The cells were then incubated for 72 h and proliferation was monitored by measuring (^{3}H)-thymidine incorporation. Data are presented as percent inhibition of (^{3}H)-thymidine incorporation observed in control cultures (Con A alone; (44,490 cpm)). Results represent the mean ± SD of three experiments each performed in triplicate. Inset shows SDS-PAGE analysis of the purified Sip.

0.1% sodium citrate and 0.1% Triton X-100 for 2 min on ice. The TUNEL reaction was carried out using the In situ Cell Death Detection kit, (Roche Diagnostic Co., Indianapolis, IN) according to manufacturer's directions. Cells were analyzed by flow cytometry as previously described (33). To measure caspase activation, cells were harvested, exposed to FAM-VAD-FMK (CaspaTag® Fluorescein Caspase Activity kit; Intergen Co., Purchase, NY) and incubated in the dark for 1 h at 37°C. The cells were washed and analyzed by flow cytometry. FAM-VAD-FMK fluorescence was excited by an argon laser operating at 488 nm and excitation measured with a 530-nm bandpass filter using log amplification.

Results

We previously reported that crude sonic extracts of *T. denticola* strain LL2513 contain a protein capable of inhibiting human T-cell activation by both antigens and mitogens (32). This spirochete immunomodulatory protein, designated Sip, was partially purified using a combination of ion exchange, chromatofocusing, and gel filtration chromatography. The enriched preparation of Sip consists of two peptides of approximately 50 and 56 kDa (Fig. 1, inset). The two Sip peptides appear to be equimolar in the purified preparation; it should also be noted that only one band was observed under non-denaturing electrophoretic conditions (data not shown). Human lymphocytes exposed to varying amounts of Sip (0–0.5 μg protein/ml) exhibit a dose-dependent reduction in their ability to proliferate in response to Con A (Fig. 1). In the presence of 0.12 μg/ml of Sip, (^{3}H)-thymidine incorporation was inhibited 32.7%; inhibition increased to 52.9% and 74.4% in the presence of 0.25 μg/ml and 0.5 μg/ml of Sip, respectively.

In addition to (^{3}H)-thymidine incorporation, propidium iodide in conjunction with flow cytometry was employed to assess cell cycle progression in Sip-treated cells. As shown in Fig. 2(A), 97.3% of lymphocytes incubated in medium alone were found in the G_0/G_1 phase of the cell cycle. Treatment with PHA led to entry of cells into the cell cycle (Fig. 2B); 58.0% of the cells were in the G_0/G_1 phase, 34.6% in the S phase, and 7.4% in the G_2/M phase. In contrast, cells pre-exposed to 0.25 μg/ml of Sip were blocked from entering the S, and G_2/M phases; 75.1% of the cells were in the G_0/G_1 phase, 19.9% in the S phase and 5.0% in the G_2/M phase (Fig. 2C). Inhibition of cell cycle progression was further exacerbated by exposure to 0.5 μg/ml Sip; 87.7% of the cells were in the G_0/G_1 phase, 8.6% in the S phase and 4.6% in the G_2/M phase (Fig. 2D). To determine if cells were activated in the presence of Sip, we needed to distinguish between the G_0 and G_1 phases. Therefore, we next conducted dual parametric cell cycle analysis in which DNA content was assessed using Hoechst 33342 fluorescence along with total protein (FITC fluorescence) or total RNA (pyronin Y fluorescence) content. As shown in Fig. 3(A), 90.1% of cells incubated in medium alone remain in the G_0 phase, which is characterized by diploid DNA content (dim Hoechst 33342 fluorescence) and low protein content (dim FITC fluorescence). In contrast, PHA activation leads to a distribution in which cells were found in all phases of the cell cycle; 56.3% in the G_0 phase, 17.7% in the G_1 phase (diploid DNA content and increased FITC fluorescence), 14.7% in the S phase and 11.3% in the G_2/M phase (high Hoechst 33342 and FITC fluorescence (Fig. 3B)). In the presence of Sip, 58.7% of the cells were found in the G_0 phase and 31.2% in the G_1 phase; the remainder of the cells (9.1%) were distributed among the S and G_2/M phases (Fig. 3C). Analysis of DNA (Hoechst 33342) and RNA content (pyronin Y) showed a similar pattern of cell cycle distribution. Non-activated lymphocytes (medium only) were found primarily in the G_0 phase ((92.7%); Fig. 3(D); PHA activation led to 45.0% of the cells in the G_1 phase, 12.4% in the S phase, and 14.8% in the G_2/M phase (Fig. 3E). In contrast, PHA activation in the presence of Sip resulted in 36.8% in the G_0 phase, 52.9% in the G_1 phase and 5.1% and 5.2% in the S and G_2/M phases, respectively (Fig. 3F).

The preceding experiments suggest that in the presence of Sip, lymphocytes are indeed activated by PHA; however, the cells are not able to progress beyond the G_1 phase of the cell cycle. To further demonstrate that cells were activated in the presence of Sip and progressed from G_0 to the G_1 phase, we assessed other events associated with this phase of lymphocyte activation. Specifically, we focused on the expression of two proteins associated with transition through the G_1 phase of the cell cycle; the activation inducer molecule, CD69, and the interleukin-2 receptor (IL-2R), CD25. As shown in Fig. 4(B,E), PHA-activated T-cells exhibit increased expression of CD69 (73.2%) and CD25 (52.3%). This compares with 6.5%

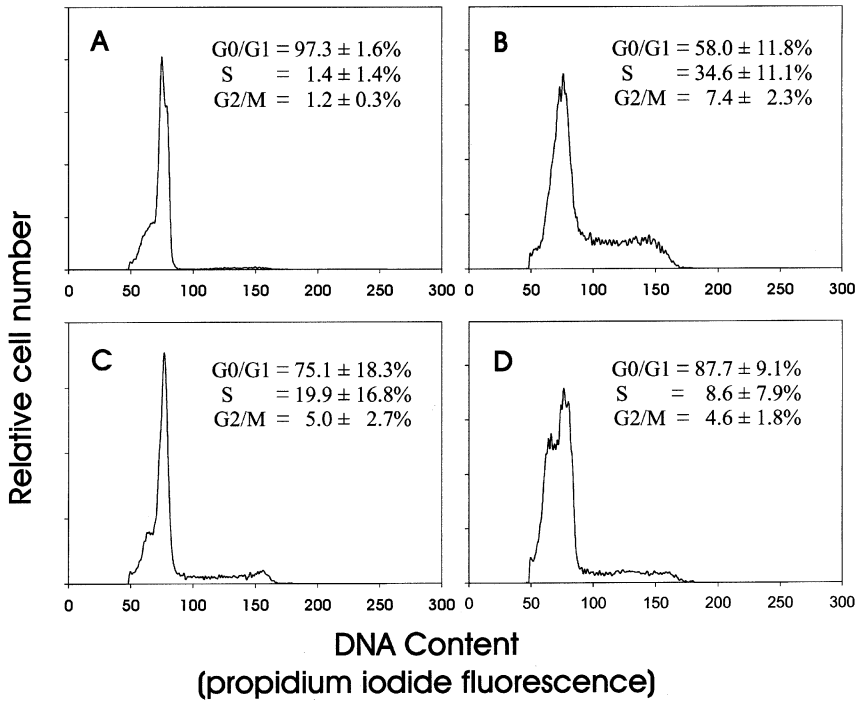

Fig. 2. Cell cycle analysis of Sip-treated cells. HPBMC were incubated with medium alone (panel A), PHA (panel B), PHA and Sip (0.25 μg protein/ml; (panel C)) or PHA and Sip (0.5 μg/ml; (panel D)) for 72 h. The cells were then stained with propidium iodide as described in Materials and methods. Cell cycle analysis was performed by flow cytometry; at least 10,000 cells were assessed per sample. Numbers in each panel represent the mean ± SD for cell cycle distribution (%) of five experiments each performed in triplicate.

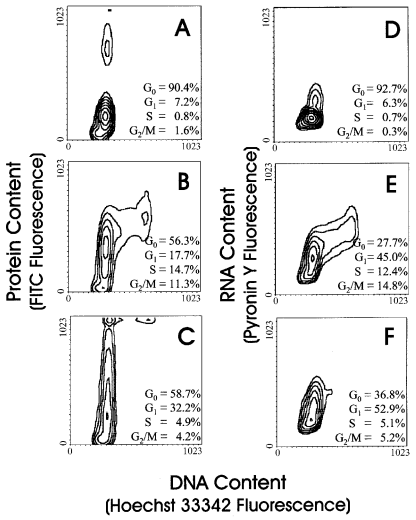

Fig. 3. Dual parameter cell cycle analysis of Sip-treated cells. Lymphocytes were incubated with medium alone (panels A and D), PHA (panels B and E), or PHA and 0.25 μg protein/ml of SIP (panels C and F) for 72 h. Cells were then stained with Hoechst 33342 and FITC (panels A–C) or pyronin Y (panels D–F) and analyzed by flow cytometry as described in Materials and methods. Results are displayed as contour plots and are representative of three experiments; 10,000 cells were analyzed per sample. The percentage of cells in each phase of the cell cycle is indicated in the panels.

(CD69) and 6.4% (IL-2R) in non-activated cells (Fig. 4A,D). Sip failed to influence the percentage of lymphocytes expressing these activation markers; 84.1% and 65.3% of the cells expressed CD69 and CD25, respectively (Fig. 4C,F). The level of CD69 and CD25 expression in Sip-treated cells was also comparable to that of PHA-treated cells; the mean channel fluorescence was 307.6 (CD69) and 81.5 (CD25) for PHA-treated cells and 238.0 (CD69) and 87.5 (CD25) for Sip-treated cells.

In a final series of experiments, we focused on the fate of Sip-treated cells by determining whether lymphocytes become apoptotic following exposure to the immunoinhibitory protein. Apoptosis was assessed by analyzing cells for two hallmarks of this form of cell death: DNA fragmentation and caspase activation. DNA fragmentation was measured using the TUNEL assay. As shown in Fig. 5(A) and 9.6% of cells treated with PHA alone exhibit DNA fragmentation; in contrast, DNA fragmentation was detected in 39.6% of Sip-treated cells (Fig. 5B). Caspase activation was assessed using the fluorescent tripeptide caspase inhibitor, FAM-VAD-FMK, which binds to the active site of several activated caspases (caspase-1, -2, -3, -4, -5, -6, -7, -8 and -9). In the presence of PHA, 24.0% of the

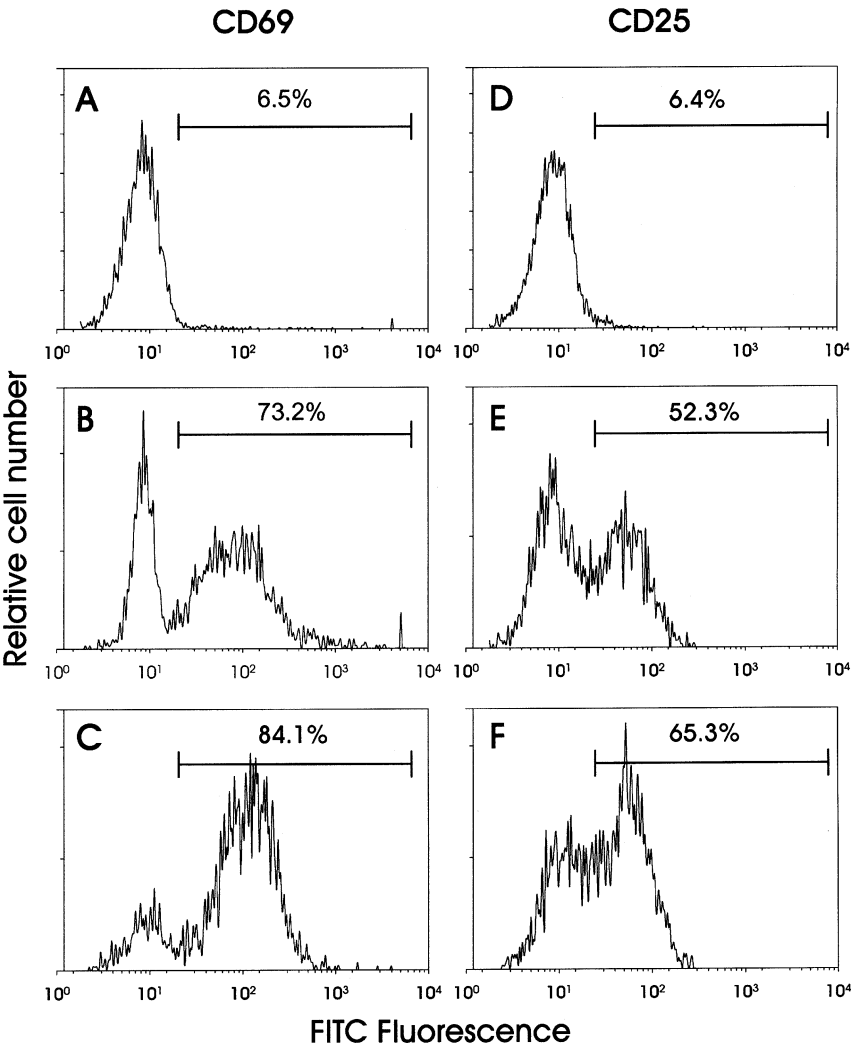

Fig. 4. Effect of Sip on lymphocyte expression of CD69 and CD25. Lymphocytes were incubated with medium (panels A and D), PHA (panels B and E), or PHA and 0.25 μg/ml of Sip (panels C and F) for 24 h; the cells were stained with anti-CD69 (panels A–C) or anti-CD25 (panels D–F) monoclonal antibodies conjugated to FITC and analyzed by flow cytometry. The numbers in each panel represent the percentage of positive cells; analysis gates were set so that >98% of cells stained with isotypic control antibodies remained outside the positive region. Results are representative of three experiments; at least 10,000 cells were analyzed per sample.

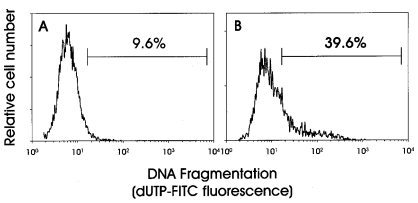

Fig. 5. Assessment of DNA fragmentation. HPBMC were treated with PHA (panel A) or PHA and 0.25 μg protein/ml of Sip (panel B) and incubated for 96 h. DNA fragmentation was measured using the TUNEL assay (dUTP-FITC fluorescence). The numbers in each panel represent the percentage of cells exhibiting DNA fragmentation and are representative of three experiments; 5000 cells were assessed per sample.

lymphocytes contained activated caspases (Fig. 6A); caspase activation increased to 49.2% in the presence of Sip (Fig. 6B). It should be noted that Sip-induced apoptosis was observed at 96 h. No significant difference in cell death was observed between the Sip-treated cells and the PHA control cells at earlier time points (data not shown).

Discussion

In this study we have demonstrated that a highly enriched preparation of Sip induces a dose-dependent inhibition of mitogen-induced lymphocyte (^{3}H)-thymidine incorporation. Furthermore, cell cycle analysis

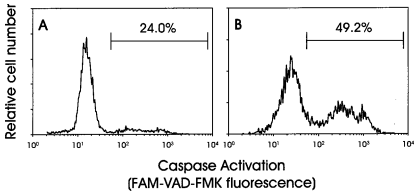

Fig. 6. Assessment of caspase activation. HPBMC were incubated for 96 h in the presence of PHA (panel A) or PHA and 0.25 μg protein/ml of Sip (panel B). Caspase activation was monitored by flow cytometry after staining with the caspase inhibitor FAM-VAD-FMK. Data are plotted as caspase activation (FAM-VAD-FMK fluorescence) versus relative cell number. The numbers in each panel represent the percentage of positive cells and are representative of three experiments; 5000 cells were assessed per sample.

indicates that Sip-treated lymphocytes remain in the G_0/G_1 phase of the cell cycle. It is noteworthy that the single parametric method initially employed for cell cycle analysis did not enable us to distinguish between the G_0 and G_1 phases. However, by employing dual parameter cell cycle analysis based upon DNA content along with either total RNA or protein levels, we were able to demonstrate that Sip-treated cells do indeed enter the cell cycle (G1 phase), but fail to progress into the S phase resulting in the accumulation of cells in the G_1 phase. Sip-induced G_1 arrest was further demonstrated by monitoring the expression of the cell activation markers, CD69 and CD25, which are upregulated as cells pass through the early to mid-G_1 phase of the cell cycle. Our results demonstrate that both CD69 and CD25 are expressed in cells exposed to Sip at levels comparable to PHA control cultures. Collectively, these data support the conclusion that lymphocytes are activated in the presence of Sip but are unable to progress beyond the G1 phase of the cell cycle.

It is becoming increasingly evident that perturbation of the cell cycle of host cells is a common target utilized by a number of pathogens. For instance, *Helicobacter pylori* (34) has been shown to inhibit the G_1 to S transition of gastric epithelial cells. Likewise, we have demonstrated that *F. nucleatum* produces an immunoinhibitory protein that induces a mid-G_1 phase arrest of human lymphocytes. Furthermore, the G_1 arrest is associated with the failure to express cyclin D3 and PCNA (29). Another bacterial toxin, produced by *Haemophilus ducreyi,* induces fibroblasts to arrest in the G_1 phase of the cell cycle (5); the mechanism for the arrest has not been determined. Furthermore, the family of cytolethal distending toxins produced by *A. actinomycetemcomitans, Escherichia coli, H. ducreyi* and *Campylobacter jejuni* induces G_2 arrest in human T cells and other cell lines (4, 6, 33, 39). Preliminary studies suggest that the G_2 arrest is linked to activation of the G_2 checkpoint and is irreversible, culminating in activation of the apoptotic cascade.

We have not determined the precise mechanism by which Sip induces G_1 arrest. However, progression through the cell cycle is regulated by the temporal activation of a family of related protein kinases, the cyclin-dependent kinases ((cdk), reviewed in (7) and (25)). While the activity of these kinases normally fluctuates in a tightly regulated fashion throughout the cell cycle, the absolute amount of protein remains relatively constant. Instead, cdk activity is regulated by the availability of cyclin partners, and in some instances, dephosphorylation of the kinase itself. With regards to the G_1 phase, progression through this phase requires activation of cdk4 and cdk2. Cdk4 activation regulates transit through mid to late-G_1; this kinase requires the availability of the D family of cyclins and PCNA to form an active complex. Likewise, cdk2, which regulates the late G_1 phase and transit into the S phase, requires cyclin E and PCNA. Failure to express adequate levels of PCNA and the G_1 cyclins in a timely fashion impairs the ability of cells to complete the cell cycle and results in G_1 arrest. Indeed, preliminary results indicate that Sip-treated cells exhibit reduced expression of cyclins D3, E and PCNA.

Delays in cell cycle progression, known as checkpoints, occur at discrete points: G_1-S boundary, G_2-M boundary and in the S phase as well (23, 27). The checkpoints are governed by a series of control systems which are most commonly activated by DNA damage. The purpose of these checkpoints is to delay the cell cycle and allow DNA repair to occur. The G_1 checkpoint consists primarily of p53 and p21; the latter protein is a potent cdk inhibitor. Following DNA damage, p53 levels increase as a result of protein stabilization. This leads to increased expression of p21, which in turn binds to cdk and inhibits the active complex. Inactivation of cdk leads to reduced phosphorylation of Rb and results in G_1 arrest (reviewed in 11, 23, 27). The p21 peptide may also bind to PCNA, which serves as a component of DNA polymerase I. This implies that p21 has a dual role, as a critical component of the G_1 checkpoint as well as of the DNA repair apparatus. If cells are unable to repair DNA damage, then the checkpoint prevents them from re-entering the cell cycle and instead may lead to activation of the apoptotic cascade. Alternatively, if cells are able to repair DNA, they may then be released to complete the cell cycle.

We have not determined if Sip directly (or indirectly via DNA damage) activates the G_1 checkpoint. Instead, we studied the fate of G_1-arrested cells by determining if they undergo apoptosis. We first determined that Sip-treated cells exhibit DNA fragmentation; this was not observed until 96 h after exposure to the inhibitory protein whereas maximal G_1 arrest was detected at 72 h. Thus it appears that G_1 arrest precedes activation of the apoptotic cascade. DNA fragmentation represents the results of a series of upstream events associated with apoptosis and occurs relatively late in the death process. Therefore, we also assessed Sip-treated cells for earlier apoptotic events such as caspase activation. Indeed, we show that the family of cysteine-aspartic acid specific proteases are activated in cells 96 h following treatment with Sip. In this study, we utilized a tripeptide inhibitor, FAM-VAD-FMK to measure caspase activation. This inhibitor enters the cell and irreversibly binds to activated caspases; however, this inhibitor is not caspase specific and is able to detect several activated caspases including caspases -1, -2, -3, -4, -5, -6, -7, -8 and -9 (2). In preliminary experiments, however, we have utilized specific caspase inhibitors and determined that caspases -8, -9, and -3 are activated in Sip-treated cells. Activation of caspase-8 leads to perturbation of mitochondrial function and translocation of cytochrome c to the cytosol. Cytochrome c normally resides in the intermembrane space of the mitochondria and its release into the cytosol is linked to the development of the mitochondrial permeability transition state and the activation of downstream caspases -9 and -3 (12, 18, 41). Collectively, our data indicate that Sip-induced G_1 arrest is followed by cell death. Thus, we infer that Sip-induced G_1 arrest leads to activation of the G_1-S checkpoint and irreversible cell cycle arrest.

There is increasing evidence that the host immune system is a target of many human pathogens. Avoidance or modulation of the immune response by pathogens may be a critical event in determining the outcome of numerous infectious processes. Bacterially derived immunosuppressive factors, such as Sip, could lead to a state of hyporesponsiveness that favors establishment or colonization by the initiating organism or by other opportunistic organisms. As previously mentioned, *T. denticola* has been implicated in the

pathogenesis of several diseases and is also considered to be an opportunistic organism infecting compromised patients. Our data demonstrate that Sip acts as an immunotoxin by disrupting the ability of T- cells to properly progress through the cell cycle; the arrested cells eventually become apoptotic. This disturbance could, in turn, adversely affect the development of normal immunologic defense mechanisms. We propose that such immunologic perturbation could contribute to the pathogenesis of diseases associated with *T. denticola* infection.

Acknowledgments

The authors wish to thank Terry McKay and Rose Espiritu for their expert technical assistance and the SDM Flow Cytometry Facility for its support of these studies. This work was supported by the USPHS grant DE14191.

References

1. Armitage GC, Dickinson W, Jenderseck R, Levine S, Cahmbers D. Relationship between the percentage of subgingival spirochetes and the severity of periodontal disease. J Periodontol 1982: **53**: 550–556.
2. Bedner E, Smolewski P, Amstad P, Darzynkiewicz Z. Activation of caspases measured *in situ* by binding of fluorochrome-labeled inhibitors of caspases (FLICA). Correlation with DNA fragmentation. Exp Cell Res 2000: **259**: 308–313.
3. Chan E, McLaughlin R. Taxonomy and virulence of oral spirochetes. Oral Microbiol Immunol 2000: **15**: 1–9.
4. Comayras C, Tasca C, Peres SY, Ducommun B, Oswald E, De Rycke J. *Escherichia coli* cytolethal distending toxin blocks the HeLa cell cycle at the G2/M transition by preventing cdc2 protein kinase dephosphorylation and activation. Infect Immun 1997: **65**: 5088–5095.
5. Cope L, Lumbley SLJ, Klesney-Tait J, Stevens M, Johnson L, Purven M, Munson R, Lagergard T, Radolf J, Hansen E. A diffusible cytotoxin of *Haemophilus ducreyi*. Proc Natl Acad Sci USA 1997: **94**: 4056–4061.
6. Cortes-Bratti X, Chaves-Olarte E, Lagergard T, Thiagalingam S. The cytolethal distending toxin from the chancroid bacterium *Haemophilus ducreyi* induces cell cycle arrest in the G2 phase. J Clin Invest 1999: **103**: 107–115.
7. Doree M, Galas S. The cyclin-dependent protein kinases and the control of cell division. FASEB J 1995: **8**: 1114–1121.
8. Engers HD, Louis JA, Zubler RH, Hirt B. Inhibition of Tx cell-mediated functions by MVM (i), a parvovirus closely related to minute virus of mice. J Immunol 1981: **127**: 2280–2285.
9. Floersheim GL, Hopff WH, Gasser M, Bucher K. Impairment of cell mediated immune response by *Pseudomonas aeruginosa*. Clin Exp Immunol 1971: **9**: 241–247.
10. Hanna EE, Watson DW. Host-parasite relationships among group Z streptococci. IV. Suppression of antibody response by streptococcal pyrogenic exotoxin. J Bacteriol 1968: **90**: 14–21.
11. Hartwell LH, Kastan MB. Cell cycle control and cancer. Science 1994: **266**: 1821–1828.
12. Hirsch T, Marchetti P, Susin SA, Dallaporta B, Zamzami N, Marzo I, Geuskens M, Kroemer G. The apoptosis-necrosis paradox. Apoptogenic proteases activated after mitochondrial permeability transition determine the mode of cell death. Oncogene 1997: **15**: 1573–1581.
13. Holmgren J, Lindholm L, Lonnroth I. Interaction of cholera toxin and toxin derivatives with lymphocytes. I. Binding properties and interference with lectin-induced cellular stimulation. J Exp Med 1974: **139**: 801–819.
14. Ishihara K, Okuda K. Molecular pathogenesis of the cell surface proteins and lipids from *Treponema denticola*. FEMS Microbiol Lett 1999: **181**: 199–204.
15. Kantzler GB, Lauteria SF, Cusumano CL, Lee JD, Ganguly R, Waldman RH. Immunosuppression during influenza virus infection. Infect Immun 1974: **10**: 996–1002.
16. Kauffman CA, Phair JP, Linnemann CC, Jr, Schiff GM. Cell-mediated immunity in humans during viral infection: I. Effect of rubella on dermal hypersensitivity, phytohemagglutinin reponse, and T lymphocyte numbers. Infect Immun 1974: **10**: 212–215.
17. Khansari N, Segre M, Segre D. Immunosuppression in murine malaria: a soluble immunosuppressive factor derived from *Plasmodium berghei*-infected blood. J Immunol 1981: **127**: 1889–1893.
18. Kroemer G. The mitochondrion as an integrator/coordinator of cell death pathways. Cell Death Differ 1998: **5**: 547.
19. Listgarten MA. Colonization of subgingival areas by motile rods and spirochetes: clinical implication. In: Genco RJ, Mergenhangen SE, editors. Host-Parasite Interaction in Periodontal Diseases. Washington, D.C.: American Society of Microbiology, 1982: 112.
20. Loesche WJ. The role of spirochetes in periodontal disease. Adv Dent Res 1988: **2**: 275–283.
21. Malakian AH, Schwab JH. Biological characterization of an immunosuppressant from group A streptococci. J Exp Med 1971: **134**: 1253–1265.
22. Nair PNR. Light and electron microscopic studies of root canal flora and periapical lesions. J Endod 1987: **13**: 29–39.
23. O'Connor PM. Mammalian G1 and G2 phase checkpoints. Cancer Surv 2000: **29**: 151–182.
24. Olson GB, Dent PB, Rawls WE, South MA, Montgomery JR, Melnick JL, Good RA. Abnormalities of *in vitro* lymphocyte responses during rubella virus infections. J Exp Med 1968: **128**: 47–68.
25. Pines J. Cyclins and their associated cyclin-dependent kinases in the human cell cycle. Biochem Soc Trans 1993: **21**: 921–925.
26. Sato T, Kuramitsu H. Polymerase chain reaction for the detection of *flaA*-1 genes of oral spirochetes in human advanced periodontal pockets. Arch Oral Biol 2000: **45**: 925.
27. Shapiro GI, Harper JW. Anticancer drug targets: cell cycle and checkpoint control. J Clin Invest 1999: **104**: 1645–1653.
28. Shenker BJ. Immunologic dysfunction in the pathogenesis of periodontal diseases. J Clin Periodontol 1987: **14**: 489–498.
29. Shenker BJ, Datar S. *Fusobacterium nucleatum* inhibits human T-cells by arresting cells in the mid G_1 phase of the cell cycle. Infect Immun 1995: **63**: 4830–4836.
30. Shenker BJ, McArthur WP, Tsai CC. Immune suppression induced by *Actinobacillus actinomycetemcomitans*. I. Effects on human peripheral blood lymphocyte responses to mitogens and antigens. J Immunol 1982: **128**: 148–154.
31. Shenker BJ, Tsai C-C, Taichman NS. Suppression of lymphocyte responses by *Actinobacillus actinomycetemcomitans*. J Periodontal Res 1982: **17**: 462–465.
32. Shenker BJ, Listgarten MA, Taichman NS. Suppression of human lymphocyte responses by oral spirochetes: a monocyte-dependent phenomenon. J Immunol 1984: **132**: 2039–2045.
33. Shenker BJ, Hoffmaster RH, Zekavat A, Yamguchi N, Lally ET, Demuth DR. Induction of apoptosis in human T cells by *Actinobacillus actinomycetemcomitans* cytolethal distending toxin is a consequence of G_2 arrest of the cell cycle. J Immunol 2001: **167**: 435–441.
34. Shirin H, Sordillo EM, Oh SH, Yamamoto H, Delohery T, Weinstein IB. *Helicobacter pylori* inhibits the G_1 to S transition in AGS gastric epithelial cells. Cancer Res 1999: **59**: 2277–2281.
35. Siqueira FJ Jr, Rocas IN, Favieri A, Santos KRN. Detection of *Treponema denticola* in endodontic infections by 16S rRNA gene detected polymerase chain reaction. Oral Microbiol Immunol 2000: **15**: 335–337.
36. Siqueira FJ Jr, Rocas IN, Oliveira JCM, Santos KRN. Detection of putative oral pathogens in acute periradicular abscesses by 16S rDNA-directed polymerase chain reaction. J Endod 2001: **27**: 164–167.
37. Thilo B, Baehni P, Holz J, Baume LJ. Distribution des bacteries dans les parties coronaire et apicale de dents a pulpe necrosee. SSO: Schweizerische Monatsschrift fur Zahnheilkunde 1983: **93**: 335–350.
38. Wang Q, Ko K, Kapus A, McCulloch A, Ellen RP. A spirochete surface protein uncouples store-operated calcium channels in fibroblasts. J Biol Chem 2001: **276**: 23056–23064.
39. Whitehouse CA, Balbo P, Peter ME, Cottle DL, Mirabito P, Pickett CL. *Campylobacter jejuni* cytolethal distending toxin causes a G2 phase cell cycle block. Infect Immun 1998: **66**: 208–212.
40. Yoshida H, Jontell M, Sundqvist G, Bergenholtz G. Effect of sonicated material from *Fusobacterium nucleatum* on the functional capacity of accessory cells derived from dental pulp. Oral Microbiol Immunol 1995: **10**: 208–212.
41. Zamzami N, Hirsch T, Dallaporta B, Petit PX, Kroemer G. Mitochondrial implication in accidental and programmed cell death: apoptosis and necrosis. J Bioenerg Biomembr 1997: **29**: 185–193.